DR STEPHEN P. LONG (Orcid ID : 0000-0002-8501-7164)

Article type : Special Issue Article

Photosynthesis in the fleeting shadows: An overlooked opportunity for increasing crop productivity?

Yu Wang[1] (0000-0002-6951-2835), Steven J. Burgess (0000-0003-2353-7794)[1], Elsa de Becker[1,2](0000-0002-7928-2586), Stephen P. Long (0000-0002-8501-7164) [1,3,4*]

[1] Carl R Woese Institute for Genomic Biology, University of Illinois at Urbana-Champaign, Urbana, IL, 61801, USA

[2] Department of Plant Biology, University of Illinois at Urbana-Champaign, Urbana, IL 61801, USA.

[3]Department of Crop Sciences, University of Illinois at Urbana-Champaign, Urbana, IL 61801, USA.

[4] Lancaster Environment Centre, Lancaster University, Lancaster, LA1 4YQ, UK

*e-mail address of corresponding author: slong@illinois.edu

Chronos Reference: ED6E4EB9-BDC3-4815-8786-9034A52ADA15

Running head: Photosynthesis in the shadows

Keywords: Photosynthetic induction, non-photochemical quenching, NPQ, food security, soybean, wheat, photosystem II, photoinhibition , stomata, crop breeding, leaf canopy, Rubisco activase

Summary

Photosynthesis measurements are traditionally taken under steady-state conditions. However, leaves in crop fields experience frequent fluctuations in light and take time to respond. This slow response reduces the efficiency of carbon assimilation. Low to high light transitions require photosynthetic induction, including the activation of Rubisco and opening of stomata, while high to low light transitions require relaxation of dissipative energy processes collectively known as non-photochemical quenching (NPQ). Previous attempts to assess the impact of these delays on net carbon assimilation have used simplified models of crop canopies, limiting the accuracy of predictions. Here we use ray tracing to predict the spatial and temporal dynamics of lighting of a rendered mature soybean canopy to review the relative importance of these delays on net cumulative assimilation over the course of both a sunny and a cloudy summer day. Combined limitations result in a 13 % reduction in crop carbon assimilation on both sunny and cloudy days, with induction more important on cloudy than sunny days. Genetic variation in NPQ relaxation rates and photosynthetic induction in parental lines of a soybean nested association mapping (NAM) population were assessed. Short-term NPQ relaxation (<30 min) showed little variation across the NAM lines, but substantial variation was found in speeds of photosynthetic induction, attributable to Rubisco activation. Over the course of a sunny and an intermittently cloudy day these would translate to substantial differences in total crop carbon assimilation. These findings suggest an unexplored potential for breeding improved photosynthetic potential in our major crops.

Introduction

Improvement of crop photosynthesis for yield increases has focused on rates of leaf CO_2 uptake at light-saturation (A_{sat}) and under constant light. No correlation between variation in A_{sat} and yield was found across a selection of modern wheat accessions (Rawson *et al.* 1983). Further, wild ancestors of wheat showed higher A_{sat} than elite cultivars (Dunstone *et al.* 1973). Such influential early findings led to skepticism that photosynthesis can be improved in crops, and this view persists with some today despite evidence that bioengineered increases in steady-state photosynthesis do correspond to significant increases in productivity (Köhler *et al.* 2016, Sinclair

et al. 2019, South *et al.* 2019). However, under field conditions light in a crop canopy is rarely constant. Fluctuations result from intermittent cloud cover, but more importantly from the continuous change in sun angle over the day causing intermittent shadowing within the canopy by overlying leaves and other plant structures (Wang *et al.* 2017b, Zhu *et al.* 2004). Might we therefore have overlooked a major opportunity by focusing on steady-state photosynthesis?

A dynamic light environment impacts photosynthesis in two main ways: A leaf in the shade of another receives about 1/10 th of the light of one in full sun (Zhu et al., 2004). These periods of full sun and of shade may last seconds to hours (Deans *et al.* 2019, Tanaka *et al.* 2019, Zhu, et al. 2004). Using reverse ray-tracing, and assuming a random distribution of leaves, Zhu et al. (2004) showed that even on a clear day, leaves in a static canopy will experience over 20 sun-shade-sun transitions. When leaves move into full light after a period of shade, leaf CO_2 uptake rate (*A*) does not instantly reach its maximum value, but rises gradually over several minutes to approach a new steady state. This has been termed photosynthetic induction, and it causes a substantial reduction in the efficiency of carbon fixation (Salter *et al.* 2019, Soleh *et al.* 2017, Taylor and Long 2017, Yamori *et al.* 2012). Secondly, leaves in full sunlight receive more energy than they can use, leading to the activation of non-photochemical quenching (NPQ) which dissipates excess energy as heat. This reduces the production of oxidizing radicals via excited-state chlorophyll molecules that would damage the photosynthetic apparatus. On a sun to shade transition there is similarly a loss of potential CO_2 assimilation. This is because various components of NPQ have relaxation half-lives of seconds to hours, the leaf therefore continues dissipating light as heat even after it is moved into the shade, where it could use all received light in photosynthesis. This forces *A* below the steady-state level that it will eventually resume. Practical proof of the importance of this was shown with a bioengineered increase in the rate of dissipation of NPQ during sun-shade transitions. This resulted in a doubling of *A* in fluctuating light and a significant increase in tobacco productivity in replicated-plot field trials (Kromdijk *et al.* 2016). Many NPQ components have been identified so far, such as energy-dependent quenching qE (Krause et al., 1982), Zeaxanthin dependent quenching qZ (Dall'Osto et al., 2005, Nilkens et al., 2010), chloroplast relocation dependent quenching qR (Cazzaniga et al., 2013), state transition dependent quenching qT

(Nilkens et al., 2010), photoinhibition quenching qI and photoinhibition-independent sustained quenching qH (Malnoë et al., 2018), although the relative contribution of these processes may depend on conditions and species.

It has been argued that evolution and breeder selection would have already optimized photosynthesis in our crops (Winer 2019). Two factors, with respect to photosynthesis in fluctuating light, counter this argument. First, the ancestors of our major crops evolved in relatively open habitats that could support the production of few leaves, hence both shading and self-shading would have been rare. For example, in the case of soybean, the wild ancestor is an annual twining vine that climbs on other stems and spaces its leaves to largely avoid shading. In contrast, today's elite cultivars have been bred as bush forms, grown at densities where they will form 5-7 m^2 of leaf area over every m^2 of field. In essence, the leaves of what were sun plants by origin are now grown so that most leaves are shaded or intermittently shaded. Given the speed at which crop planting density has increased for our major crops, there is good reason to expect that neither evolution nor breeder selection have kept pace. Indeed two major crops have now been shown to fail to adapt to shading such that canopy photosynthesis is optimized (Pignon *et al.* 2017). Second, current [CO_2] and light levels are co-limiting to photosynthesis in C3 crops. Atmospheric [CO_2] has risen from the 220 ppm average of the past 25 M years to 407 ppm in 2018, with half of that increase occurring in just the last 60 years. This means light has become progressively more limiting and CO_2 progressively less limiting, strongly affecting photosynthetic efficiency in the shade (Long *et al.* 2004). Again, there is likely insufficient time for adaptation to this change. This may be reflected in the large variation in speeds of induction on shade to sun transitions within germplasm of cassava, rice, soybean and wheat (Acevedo-Siaca *et al.* 2020, De Souza *et al.* 2019, Salter, et al. 2019, Soleh, et al. 2017). For example, the between accession variation in CO_2 assimilated during the induction was three times that of steady-state assimilation in cassava (De Souza, et al. 2019), suggesting that optimization of photosynthesis in fluctuating light has not occurred.

Because of fluctuations in light the leaf transiently forgoes potential assimilation compared with that which would be achieved with an instantaneous response of photosynthesis (Deans, et al.

2019, Taylor and Long 2017, Zhu, et al. 2004). Over the course of a day, how much potential photosynthesis does a crop canopy forgo? Two recent estimates predicted a daily loss for wheat of up to 15 – 21 % (Salter, et al. 2019, Taylor and Long 2017). However, these estimates did not use realistic canopy models, simulated only small parts of the canopy and did not consider the combined effect of shade-sun and sun-shade transitions. More accurate assessments of these efficiency losses during light fluctuations require representation of actual crops and the dynamic spatial and temporal dynamics of lighting across all leaves in the canopy.

Using soybean as an example, here the structure of an actual canopy of an elite cultivar is combined with forward ray-tracing to predict the spatial dynamics of lighting across the entire canopy throughout the course of a clear sky and an intermittently cloudy day. This dynamic lighting is combined with kinetics of both induction of photosynthesis and NPQ relaxation to quantitatively review the losses that result compared to an instantaneous return to steady-state photosynthetic rates on light transitions. To simplify the simulation, we divided the components of NPQ dynamics into two groups, short-term ≤30 min (STNPQ) and long-term >30 min (LTNPQ). Measured variation in both induction and STNPQ relaxation across parental lines of a nested association mapping (NAM) population of soybean is used to assess their value for breeding for increased speeds to adjustment to light fluctuations.

Results

The light absorption of a soybean canopy was simulated for a clear sky (sunny) and intermittently cloudy (cloudy) day in August using the ray tracing algorithm (Fig. 1). The diurnal light absorption for all points in the canopy were simulated over the daylight hours of the sunny (Fig. 2A) and the cloudy (Fig. 2B) day. At mid-day on the sunny day, a point on a leaf at the top of the canopy experiences full sunlight (>1000 μmol m^{-2} s^{-1}) (Fig. 2C) while all points lower in the canopy experience sunflecks (Figs. 2E and 2G). Sunflecks are seen to be highly dynamic over the course of the day, particularly in the middle layers (Fig. 2E). On an intermittently cloudy day, points on both the top leaves and those below are subject to large fluctuations in absorbed light (Fig. 2D and 2F) while little light reaches points on the bottom layer (Fig. 2F).

Net cumulative canopy assimilation (A_c) was calculated over the daylight hours of the sunny (Fig. 3A) and cloudy (Fig. 3B) day, driven by the simulated temporal and spatial dynamics of lighting of the whole canopy. Simulations of A_c compared instantaneous responses to light fluctuations, with the slower responses resulting from the delays caused by photosynthetic induction (Rca), short-term NPQ relaxation (STNPQ, including qE and qM) and long-term NPQ relaxation (LTNPQ). This quantified the loss of potential canopy carbon fixation caused by these delays. On the sunny day, a positive rate of net total carbon assimilation was observed at 7:00 and a positive rate of cumulative carbon gain continued until around 18:00, when canopy respiration was again predicted to exceed photosynthesis (Fig. 3A). Simulated differences in cumulative assimilation due to delays in adjustment to light fluctuations become evident around 8:00 and progressively amplify in cumulative carbon gain through the daylight hours (Fig. 3a). Total loss due to these delays is 13.5%, with long-term NPQ relaxation (LTNPQ) accounting for the largest part of this loss (Fig. 3a; Fig. 4). On the cloudy day, since the environmental light intensity was very low in the morning (Fig 2b), net assimilation was negative from dawn until 9:40 as total canopy respiration exceeded photosynthesis. Beyond this point the simulated differences in cumulative net assimilation due to delays in adjustment to light fluctuations progressively amplified in cumulative net assimilation until 17:00 (Fig. 3B). Total loss due to these lags was 12.5%, with short-term NPQ relaxation (STNPQ) accounting for the largest part of this loss (Fig. 3B; Fig. 4). While the simulated proportionate losses were similar on both days (Fig. 4) the absolute loss on the intermittently cloudy day, (40 mmol m^{-2}) was less than half that on the sunny day (115 mmol m^{-2}).

Partitioning cassues of simulated losses shows those due to LTNPQ to be almost twice that of STNPQ and about 2.7 times that due Rubisco activation (Fig. 4). By contrast, on the cloudy day, loss due to STNPQ is higher, contributing about 40 % of the total loss, while the loss due to rca induction is similar to that due to LTNPQ relaxation (Fig. 3b; Fig. 4).

To assess the potential impact of genotypic variation on assimilation, NPQ relaxation rates were measured for the 41 parental lines of the soybean NAM population. Variation in qE and qM across the NAM population were 40 % and 49 % between the slowest and fastest genotype. Values for these two genotypes and the average across all members of the NAM population were used in the model. The genotype with the fastest relaxation (NAM27) assimilated about 1.3 % more CO_2 across the day compared with the slowest (NAM23), and about 0.8 % more than the average on the sunny day (Fig. 5). On the cloudy day, the fastest genotype (NAM27) assimilated about 0.9 % more than average (Fig. 5) suggesting small but significant additive effects across a growing season.

Previously published measurements of photosynthetic induction in the NAM population showed large variation between genotypes in induction (Soleh et al. 2017). Time course of Rubisco activation ($\tau_{Rubisco}$) for the two genotypes representing the slowest and fastest induction rate, and a third represented the middle of this range were added here to the canopy model to simulate variation in loss caused by speed of response on the sunny and cloudy day (Fig. 6). The loss in assimilation due to Rubisco activation is up to 17.4 % for NAM8, which had the slowest Rubisco activation ($\tau_{Rubisco}$ = 1850.0 s), while NAM23, the genotype with the fastest Rubisco activation ($\tau_{Rubisco}$ =129.7 s), reduced the loss to only 2.3 % on the cloudy day and 1.9 % on the sunny day.

Discussion

Using a rendering of an actual fully developed field canopy (Fig. 1) the present study suggests that the lower efficiency of photosynthesis during light fluctuations for an elite soybean cultivar costs about 13.5 % of potential crop assimilation on both a sunny and a cloudy days in the critical pod filling phase (Fig. 4). On the simulated clear sky day, LTNPQ appears the largest cause of this loss. On the cloudy day, photosynthetic induction and LTNPQ contribute equally, and the loss due to STNPQ relaxation contributes the most at 40 % (Fig. 4). Crop biomass is about 40% carbon. Assuming then that one mole of CO_2 assimilated, net of respiration, results in 75g of biomass, then the growth loss due to the lags in adjustment of photosynthesis to light fluctuations in the canopy would be a substantial 90 kg ha^{-1} d^{-1} on the sunny day. With no mechanisms known that could allow instantaneous induction of photosynthesis on shade-sun transitions or relaxation of NPQ on sun-shade transitions, it appears unlikely that breeding or bioengineering could recover more than about half of this loss. Nevertheless, a 6.5 % increase in net photosynthetic efficiency, if translated into increased crop yields, would be exceptional. It could either provide a key part of the anticipated future need for increased yield potential to ensure global food security or, should food demand stabilize, serve to reduce the global footprint of arable agriculture (Long *et al.* 2015). How could these losses in fluctuating light be decreased?

Engineered acceleration of STNPQ relaxation has already been undertaken in tobacco by up-regulating the amounts of the two enzymes involved in the interconversion of Violaxanthin and Zeaxanthin, and the photosystem II protein, PsbS, which affects the amplitude of NPQ. This increased the quantum yield of CO_2 assimilation in fluctuating light and the rate of whole chain electron transport by ca. 50 %. In replicated field trials, biomass production was increased by 14 % - 21 %. However, this was achieved with a 50 – 100 x increase in the two enzymes and a ca. 5-fold increase in PsbS (Kromdijk et al. 2016). It would seem unlikely that this scale of diversity exists within the germplasm of a crop, suggesting that improvements on this scale might only be achieved by transgenic addition of extra copies of the relevant genes or by engineering of promoter regions to up-regulate expression. This might be confirmed by the results obtained here with the NAM population parent lines, where the gain achieved with the fastest STNPQ relaxing

line showed only a 1% improvement over the average in terms of A_c (Fig. 5). Although small, it could still have value. In 2017 soybean occupied 124 Mha of the global surface which produced 353 Mt of beans (FAOStat, 2017). As such, a 0.8% increase could mean an additional 2.8 Mt or it could release over one million hectares no longer needed for soybean production. Importantly, this increase, while small in relative terms, can potentially be gained by conventional breeding.

Given that relaxation of LTNPQ is the largest contributor to losses on the sunny day, it suggests the largest gains may be achieved by focusing on this. Several genes, in particular those involved in the repair and replacement of the photosystem II D1 protein, have been functionally implicated in the slow phase of NPQ recovery (Nixon *et al.* 2010). While the optimal targets in crops are still unclear, it will be important to see these tested in model plants. With the rapid growth of complete genomic sequences for many accessions of the major crops, genome-wide association analysis provides an approach to reveal further targets (Wang *et al.* 2017a).

What factors limit the speed of induction on a shade to sun transition? In the chloroplast, photosynthesis is limited by the build-up of Calvin cycle intermediates, in particular the CO_2 acceptor molecule ribulose 1:5 bisphoshate, and the induction of light-activated photosynthetic enzymes, in particular the activation of Rubisco by Rca. Sufficient accumulation of ribulose 1:5 bisphoshate is assumed to require ca. 60 s, while activation of Rubisco may require more than 10 min (Mott and Woodrow, 2000, Taylor and Long, 2017). At the leaf level, induction can be limited by slow stomatal opening, where full opening can require many minutes (Acevedo-Siaca, et al. 2020, De Souza, et al. 2019, Faralli *et al.* 2019, McAusland *et al.* 2016), and by mesophyll conductance which generally increases with incident light. The rate of increase in mesophyll conductance on induction is generally considered faster than both stomatal opening and Rubisco activation (Deans *et al.*, 2019), but variability between species and environmental conditions is not well defined. Several studies have inferred from modeling and *in vivo* estimation of Rubisco activity ($V_{c,max}$) that activation of Rubisco is the key limitation to the speed of induction (Mott and Woodrow 2000, Soleh, et al. 2017, Soleh et al. 2016, Taylor and Long 2017, Yamori, et al. 2012). This gains support from the observation that in wheat and soybean, intercellular [CO_2] is higher

during induction than at steady-state (Soleh, et al. 2017, Taylor and Long 2017), while the converse would be expected if stomatal opening was the dominant factor. However, in other species the speed of stomatal opening appears the dominant limitation to induction (De Souza, et al. 2019, McAusland, et al. 2016) and this may be exacerbated under stress conditions (Faralli, et al. 2019). In the current study, only activation of Rubisco by Rca was considered, so the losses due to slow induction must be considered a minimum, where slow increases in stomatal and mesophyll conductance could exacerbate losses. Tthere is already evidence that increasing the activity of Rca by up-regulation of expression increases the speed of activation (Yamori, et al. 2012) while site-directed mutagenesis has been shown a non-transgenic means to increase Rca activity (Perdomo *et al.* 2019). In addition, significant natural variation in the speed of induction has been demonstrated within germplasm of cassava, soybean and wheat (De Souza, et al. 2019, Salter, et al. 2019, Soleh, et al. 2017), providing further non-transgenic opportunities for decreasing the losses due to lower photosynthetic efficiency during induction, compared to steady-state. Simulation of this variation in our canopy model suggests that considerable gains could be achieved in soybean by conventional breeding that selects for faster rates of induction (Fig. 6).

The purpose of this work was to highlight the potential for improving crop photosynthesis under non-steady state lighting conditions. To do this we had to draw on disparate sources for model parameterization, since not all parameters were available for soybean. Additionally, some of the parameters used were measured using different protocols, such as NPQ relaxation kinetics of soybean cv. LD11-2170 and the NAM population. Therefore, the predictions here should be taken only as an indication of opportunity, and need to be further improved by better measurements and parametrization. First, the rate constant of the NPQ relaxation is possibly related to the light intensities or light intensity differences (Dall'Osto et al. 2014). Second, it is not clear how leaf position and age influence the NPQ relaxation speed. Third, long-term NPQ responses of soybean and most of the major corps have not been well defined, the correlation between LTNPQ and accumulated light input have not been validated by sufficient data. Fourth, the correlation between Rubisco activation kinetics and the light intensity is poorly defined. Thus more

integrated measurement and analysis of NPQ relaxation, Rubisco activation kinetics, stomatal opening and mesophyll conductance dynamics in the major crops will improve the model prediction and its ability to partition causes. Finally, lighting was simulated for 5 mm^2 pixels of the leaf surface. However, NPQ activation and Rubisco activation occur at the level of the chloroplast with a cross-sectional area of about 25 μm^2. As a result, the speed of light change at an individual chloroplast with change in solar angle will be faster than that simulated. Simulating smaller areas greatly increases computer time, but is likely to become practical as computational power increases. However, the compromise used here will have resulted in some under-estimation of the cost due to these light transitions.

In conclusion, this first model analysis of light fluctuations in an actual crop canopy indicates unexploited breeding and bioengineering targets to substantially improve photosynthetic efficiency and productivity. While this analysis is limited to soybean, it appears reasonable to expect similar gains in other C3 crops, including cassava, wheat and rice. While it cannot be certain that an improvement in photosynthetic efficiency will increase yield, there is evidence for all four crops that artificial increase in leaf photosynthesis by season-long elevation of [CO_2] under open-air field conditions results in highly significant increases in yield (Hasegawa *et al.* 2013, Long *et al.* 2006, Rosenthal *et al.* 2012).

Experimental procedures

3D soybean model and light distribution simulations

The dynamics of lighting within a soybean canopy were predicted with a 3D architectural representation, using our previously presented framework for crop canopies (Song *et al.* 2013, Wang, et al. 2017b). The model was parameterized on the measured architecture of a soybean (*Glycine max* L. Merr., Pioneer 93B15) crop on the University of Illinois South Farms. The leaf lengths, widths, petiole lengths and angles for trifoliate leaves of soybean (DOY 231, Aug 20) were obtained from Song et al., (2019). The canopy had a row spacing of 38 cm and plant spacing of 10 cm. The model divides the surface of each leaf into "pixels" of ca. 5 mm^2 area, which is much smaller than the "pixels" in Song et al., (2019, about 1 cm^2). To estimate light changes in the

canopy, a forward ray-tracing algorithm (FastTracer; Song et al. 2013; Wang et al. 2017b, (Song *et al.* 2019, Townsend *et al.* 2018) was used to predict the light absorption of each 5 mm^2 pixel every 1 min from 05:00 – 19:00 on Aug 20th in Champaign IL, US (40.11N, 88.21 W). At each time point the direct and diffuse light entering and within the canopy is predicted together with scattered radiation due to reflection from, and transmission through, the leaves within the canopy. Leaf reflectance and transmission were both set to 0.075 (Song et al. 2013). The sum of the direct, diffuse and scattered light incident at each pixel, less reflectance and transmission, gave the absorbed photosynthetically active photon flux density. Atmospheric transmittance was set as 0.85 to estimate the incident direct and diffuse light reaching the top of the canopy at each time point on a sunny day (Song et al., 2013). A partially cloudy day was simulated by using the measured direct and diffuse light on Aug 20th 2018 in Bondville, IL. (SURFRAD 2019). For each time point (t), the light absorption of each 5 mm^2 leaf pixel in the cloudy day ($I_{l\_c}(t)$) was calculated as:

$$I_{l\_c}(t) = I_{l\_s}(t)\,\frac{Q_{in\_c}(t)}{Q_{in\_s}(t)} \quad (1)$$

Where $I_{l\_s}(t)$ is the light absorption of each leaf pixel on the sunny day, which was calculated by the ray-tracing algorithm. $Q_{in\_s}(t)$ is the incident light above the canopy in the sunny day and $Q_{in\_c}(t)$ is the incident light above the canopy on the cloudy day, based on the actual measured incident light.

Simulation of dynamic photosynthesis

Dynamic photosynthetic rates were calculated for every 10 s (Δt) of the day using the absorbed light for each 5 mm^2 pixel, considering rates of Rubisco activation and NPQ relaxation. Account was also taken of Rubisco de-activation, since the extent of de-activation during a shade period affects the duration of induction following a return to higher light levels. Rubisco activation *in vivo* dynamics were calculated using the Rca model of Mott and Woodrow (2000) . The steady state maximum Rubisco activity (V_{cmax0_s}) was related to the amount of Rca (70 mg m^{-2}) (Mott and Woodrow 2000), where K_{aRca} is a constant in determining the maximum steady-state activity of Rubisco (Table 1)

$$V_{cmax0\_s} = \frac{V_{cmax0}[Rca]}{k_{a_{Rca}}+[Rca]} \quad (2)$$

The maximum Rubisco activity (V_{cmax}) was calculated by the following equations:

$$V_{\max\_s}(t) = V_{cmax0\_s}\frac{I_l(t)}{k_{light}+I_l(t)} \quad (3)$$

$$A_{vmax}(t) = A_{vmax}(t-\Delta t) - \Delta t \cdot \frac{(A_{vmax}(t-\Delta t) - V_{\max\_s}(t))}{\tau_{Rubisco}} \quad (4)$$

$$\mathrm{V}_{cmax}(t) = A_{Vmax}(t) \cdot \mathrm{V}_{cmax\_}0 \quad (5)$$

Where *t* time (s); $I_l(t)$ is the absorbed light of each leaf unit at time *t*. K_{light} is a constant (Table 1). $\tau_{Rubisco}$ is the time constant of Rubisco activation and de-activation; here $\tau_{Rubisco}$ is 180 s for Rubisco activation and $\tau_{Rubisco}$ is 300 s for Rubisco de-activation (Taylor and Long 2017). $A_{cmax(t)}$ is the activated proportion of Rubisco.

The short-term relaxation kinetics of non-photochemical quenching (STNPQ) was defined as the dynamics of NPQ relaxation in 30 min period, it can be described by a bi-exponential curve (Dall'Osto et al., 2014). Here qE is the fast relaxing energy dependent quenching, while qM combines all of the remaining processes up to 30 min:

$$\Phi_{NPQs}(\mathrm{t}) = N_1 I_l(t) + N_0 \quad (6)$$

$$\Phi_{qE}(t) = \Phi_{qE}(t-\Delta t) - \Delta t \cdot \frac{(\Phi_{qE}(t-\Delta t) - \Phi_{NPQs}(\mathrm{t})\cdot P_{qE})}{\tau_{qE}} \quad (7)$$

$$\Phi_{qM}(t) = \Phi_{qM}(t-\Delta t) - \Delta t \cdot \frac{(\Phi_{qM}(t-\Delta t) - \Phi_{NPQs}(\mathrm{t})\cdot P_{qM})}{\tau_{qM}} \quad (8)$$

$$\Phi_{\mathrm{NPQ}}(\mathrm{t}) = \Phi_{qE}(t) + \Phi_{qM}(t) \quad (9)$$

Where *ΦNPQs* is the steady state *ΦNPQ*, obtained from measured light response curves (see next section) of soybean (cv. LD11-2170), N_1 and N_0, which are set as 0.00028 and 0.0371, are constants calculated from measured *ΦNPQs*. P_{qE} and P_{qM} are the proportion of qE and qM. τ_{qE} and τ_{qM} are the time constants of qE and qM relaxation, separately.

Long-term non-photochemical quenching (LTNPQ), which includes, among other terms, photoinhibitory quenching (qI) and photoinhibition-independent sustained quenching (qH) decreases the maximum quantum yield of photosystem II and in turn the maximum quantum yield of CO_2 uptake (Zhu, et al. 2004). Following Zhu et al. (2004), the LTNPQ was correlated with a weighted light dose, and change in the maximum quantum yield of PSII photochemistry ($A_{Fv/Fm}(t)$) was calculated as:

$$T_f = 0.0033T^2 - 0.1795T + 3.4257 \quad (10)$$

$$I_{int}(\mathrm{t}) = \sum_{i=1}^{i=60} \frac{I_l(t-i)}{(1-\frac{i-1}{60})} \quad (11)$$

$$A_{Fv/Fm}(t) = 1 - I_{int}(t) \cdot \frac{T_f}{f_h} \quad (12)$$

Where I_{int} is the weighted light dose at time t. T_f is an empirical factor relating the relative decrease of *Fv/Fm* to temperature (*T*); *T* was set as 25 °C. f_h is an empirical constant used in determining the decrease of *Fv/Fm* for a given I_{int}. For cold-susceptible species, f_h is 5.13105.

The quantum yield of PSII was calculated as:

$$\Phi_{PSII} = A_{Fv/Fm}(t) \cdot Fv/Fm - \Phi_{NPQ}(t) \quad (13)$$

The electron transport rate, and in turn rate of leaf CO_2 uptake (*A*), is limited by the quantum yield of PSII, incident light and maximum electron transport capacity (J_{max}):

$$J = \min(\frac{1}{2}\Phi_{PSII} I(t), J_{\max}) \quad (14)$$

The rate of leaf CO_2 uptake (A) at time t was simulated by the following equations:

$$A_j(t) = \frac{(C_i - \Gamma^*) J(t)}{(4C_i + 9.3\Gamma^*)} - Rd \quad (15)$$

$$A_c(t) = \frac{V_{c\max}(t)(C_i - \Gamma^*)}{\left(C_i + K_c(1 + \frac{O_2}{K_o}\right)} - Rd \quad (16)$$

$$A(t) = \min(A_j(t), A_c(t)) \quad (17)$$

Where *Rd* is the leaf respiration. Since lower canopy leaves respire less than the upper canopy leaves, *Rd* was scaled with overlying leaf area index (LAI), as described previously (Srinivasan, et al., 2017).

$$Rd(z) = Rd_0 \exp(-kn \cdot LAI(z)) \quad (18)$$

Rd_0 is the respiration of uppermost leaf layer with a measured value of 1.2(±0.22) for soybean (cv. LD11-2170). *kn* is an exponential extinction coefficient with a measured value of 0.2 (Srinivasan, et al., 2017).

Then the canopy net CO_2 uptake (A_c) was calculated as:

$$A_c(t) = \frac{\sum(A_i(t) \cdot S_i)}{S_{ground}} \quad (19)$$

Where $A_i(t)$ is the CO_2 uptake rate of a leaf pixel; S_i is the surface area of each pixel, S_{ground} represents the occupied ground area of the simulated canopy. All simulations were conducted in MATLAB (2017b).

Measurement of dynamic NPQ parameters

To determine the kinetics of STNPQ relaxation in soybean (parameters listed in Table 2), chlorophyll fluorescence and gas exchange were measured during the transition from high light (1800 µmol m^{-2} s^{-1}) to low light (200 µmol m^{-2} s^{-1}). Measurements were taken March 9th 2019 in a controlled environmental greenhouse at the University of Illinois at Urbana-Champaign. Air temperature inside the greenhouse was set as 28 °C (day) / 24 °C (night). Leaf CO_2 uptake and

modulated chlorophyll fluorescence of the youngest fully expanded leaf was measured on 30 day-old soybean plants (cv. LD11-2170) with a gas exchange system incorporating a controlled environment leaf cuvette with a head containing a modulated chlorophyll fluorometer and LED light source (LI-6400XT and LI-6400-40; LI-COR, Lincoln, NE, USA). The measurements were made on six replicate plants. The leaves were first acclimated to dark for 30 min, with a leaf cuvette temperature (T_{block}) of 28 °C and [CO_2] of 400 µmol mol^{-1}; the light intensity was then increased to 1800 µmol m^{-2} s^{-1} for 30 min and then decreased to 200 µmol m^{-2} s^{-1} for the next 30 min, to simulate a sun-shade transition. Leaf CO_2 exchange and modulated chlorophyll fluorescence were recorded before the light was turned on, and then every 60 s for the following 60 min. Measured time series data of ΦNPQ changes represented by the following equation (Dall'Osto *et al.* 2014):

$$\Phi_{NPQ} = \Phi_{qI} + \Phi_{qE}\, e^{(-t/\tau qE)} + \Phi_{qM}\, e^{(-t/\tau qM)} \quad (20)$$

was fit with a polynomial (fit function, MATLAB 2017, The Mathworks, Inc®); fit values are listed in Table 2.

For light response curves, the leaf was dark adapted for 30 min, then it was acclimated to a light intensity of 1500 µmol $m^{-2}s^{-1}$ and a CO_2 concentration of 400 µmol mol^{-1} inside the cuvette. After 20 min, the chamber light was varied according to the following sequence: 2000, 1500, 1000, 500, 300, 200, 100 and 50 µmol $m^{-2}s^{-1}$. Chlorophyll fluorescence and gas exchange measurements were recorded after the conditions inside the cuvette regained stability at each light level, the minimal time interval was 5 min. Chlorophyll fluorescence measurements were used to calculate steady state NPQ (ΦNPQs, eqn. 6).

Variation in the rate of recovery of STNPQ quenching across the parents of the soybean NAM population.

The 41 parents of the Soybean Nested Association Mapping (NAM) population (Diers *et al.* 2018, Song *et al.* 2017) were planted at the Crop Sciences Research and Education Center at the University of Illinois at Urbana-Champaign, on June 6th 2019. The parents were planted in 1.2 m

long single-row plots with a 0.75 m row spacing. The experiment was arranged in a randomized complete block design with five replicate plots per genotype. On the 26th July, when plants were at the R1 developmental stage, three 0.48 mm leaf disks were collected from the upper-most mature leaf of each replicate plot in the field and floated on water in 24 well plates for transport back to the laboratory. Leaf disks were then laid adaxial side up on square petri dishes containing damp filter paper, sealed, wrapped in aluminum foil and incubated overnight at room temperature to allow complete relaxation of NPQ. The next day modulated photosystem II (PSII) chlorophyll fluorescence of the disks on each petri dish was imaged (FluorCam FC 800-C, PSI Systems, Czech Republic). Discs were exposed to 10 min of ~1000 µmol m^{-2} s^{-1} white light (6500 K) to induce NPQ and then 50 min of darkness. Saturating pulses (4000 µmol m^{-2} s^{-1} white light) to determine Fm' were given at 9, 40, 60, 80, 100, 120, 160, 200, 240, 300, 360, 420, 480, 540, and 598 s after the actinic light was turned on, and 1, 2, 4, 6, 8, 10, 14, 18, 22, 26, 32, 38, 44, and 50 min after the actinic light was turned off. Background was excluded automatically and NPQ values at each pulse were calculated. The maximum NPQ value for each leaf disk was set to 1, with other values normalized relative to it. Relaxation of NPQ with time was fit by non-linear least squares to equation 19 (nls function, R-project).

Simulating the effect of variation in photosynthetic induction across the NAM parent parent lines. Measured time courses of Rubisco (V_{cmax}) activation during photosynthetic induction were extracted from Soleh et al. (2017) for the NAM parent lines, using image capture and analysis software (GetData Graph Digitizer, (S.Federov, Software Publisher). Fifteen points were captured per curve for each leaf disk, then fit to an exponential function.

$$V_{cmax} = a\, e^{(-t/\tau_{Rubisco})} + c \quad (20)$$

Where $\tau_{Rubisco}$ is the time constant of Rubisco activation; c is the Rubisco activity in the dark, a is the increase of Rubisco activity from dark to light. The fitted values are listed in table 3. Then the measured $\tau_{Rubisco}$ values for NAM23, RC and NAM8 were used in this simulation. The time constant of Rubisco de-activation was assumed to be double the time required for activation for each genotype (Taylor & Long, 2017).

Data availability statement

The code and data is available at https://doi.org/10.13012/B2IDB-9453481_V1

Acknowledgments

We thank Troy Cary for setting up the soybean NAM population plots and Brian Diers for providing access to these. This work was supported by the project Realizing Increased Photosynthetic Efficiency (RIPE), that is funded by the Bill & Melinda Gates Foundation, Foundation for Food and Agriculture Research (FFAR), and the UK Department for International Development (UKAid) under grant number OPP1172157. SJB is supported by a Carl R. Woese Institute of Genomic Biology Fellowship and EdB is supported by an Illinois Distinguished Fellowship.

Author Contributions

SPL, YW and SJB designed the study. YW performed computational analysis. YW, Edb and SJB conducted STNPQ measurements. SPL, YW, SJB and EdB wrote the paper

Conflict of interest

The authors declare no conflicts of interest.

REFERENCES

Acevedo-Siaca, L.G., Coe, R., Wang, Y., Kromdijk, W., Quick, W.P. and Long, S.P. (2020) Variation in photosynthetic induction between rice accessions and its potential for improving productivity. *New Phytologist*, **accepted**.

Bernacchi, C.J., Morgan, P.B., Ort, D.R. and Long, S.P. (2005) The growth of soybean under free air [CO 2] enrichment (FACE) stimulates photosynthesis while decreasing in vivo Rubisco capacity. *Planta*, **220**, 434-446.

Dall'Osto, L., Cazzaniga, S., Wada, M. and Bassi, R. (2014) On the origin of a slowly reversible fluorescence decay component in the Arabidopsis npq4 mutant. *Philosophical Transactions of the Royal Society B: Biological Sciences*, **369**, 20130221.

De Souza, A.P., Wang, Y., Orr, D.J., Carmo-Silva, E. and Long, S.P. (2019) Photosynthesis across African cassava germplasm is limited by Rubisco and mesophyll conductance at steady-state, but by stomatal conductance in fluctuating light. *New Phytol*.

Deans, R.M., Farquhar, G.D. and Busch, F.A. (2019) Estimating stomatal and biochemical limitations during photosynthetic induction. *Plant Cell and Environment*.

Diers, B.W., Specht, J., Rainey, K.M., Cregan, P., Song, Q., Ramasubramanian, V., Graef, G., Nelson, R., Schapaugh, W. and Wang, D. (2018) Genetic architecture of soybean yield and agronomic traits. *G3: Genes, Genomes, Genetics*, **8**, 3367-3375.

Dunstone, R.L., Gifford, R.M. and Evans, L.T. (1973) PHOTOSYNTHETIC CHARACTERISTICS OF MODERN AND PRIMITIVE WHEAT SPECIES IN RELATION TO ONTOGENY AND ADAPTATION TO LIGHT. *Australian Journal of Biological Sciences*, **26**, 295-307.

FAOStat (2017) FAOSTAT. Rome, Italy: Food and Agriculture Organization of the United Nations.

Faralli, M., Cockram, J., Ober, E., Wall, S., Galle, A., Van Rie, J., Raines, C. and Lawson, T. (2019) Genotypic, Developmental and Environmental Effects on the Rapidity of g(s) in Wheat: Impacts on Carbon Gain and Water-Use Efficiency. *Frontiers in Plant Science*, **10**.

Hasegawa, T., Sakai, H., Tokida, T., Nakamura, H., Zhu, C.W., Usui, Y., Yoshimoto, M., Fukuoka, M., Wakatsuki, H., Katayanagi, N., Matsunami, T., Kaneta, Y., Sato, T., Takakai, F., Sameshima, R., Okada, M., Mae, T. and Makino, A. (2013) Rice cultivar responses to elevated CO2 at two free-air CO2 enrichment (FACE) sites in Japan. *Funct Plant Biol*, **40**, 148-159.

Köhler, I.H., Ruiz-Vera, U.M., VanLoocke, A., Thomey, M.L., Clemente, T., Long, S.P., Ort, D.R. and Bernacchi, C.J. (2016) Expression of cyanobacterial FBP/SBPase in soybean prevents yield depression under future climate conditions. *Journal of experimental botany*, **68**, 715-726.

Kromdijk, J., Glowacka, K., Leonelli, L., Gabilly, S.T., Iwai, M., Niyogi, K.K. and Long, S.P. (2016) Improving photosynthesis and crop productivity by accelerating recovery from photoprotection. *Science*, **354**, 857-861.

Long, S.P., Ainsworth, E.A., Leakey, A.D.B., Nosberger, J. and Ort, D.R. (2006) Food for thought: Lower-than-expected crop yield stimulation with rising CO2 concentrations. *Science*, **312**, 1918-1921.

Long, S.P., Ainsworth, E.A., Rogers, A. and Ort, D.R. (2004) Rising atmospheric carbon dioxide: Plants face the future. *Annual Review of Plant Biology*, **55**, 591-628.

Long, S.P., Marshall-Colon, A. and Zhu, X.G. (2015) Meeting the Global Food Demand of the Future by Engineering Crop Photosynthesis for Yield Potential. *Cell*, **161**, 56-66.

McAusland, L., Vialet-Chabrand, S., Davey, P., Baker, N.R., Brendel, O. and Lawson, T. (2016) Effects of kinetics of light-induced stomatal responses on photosynthesis and water-use efficiency. *New Phytologist*, **211**, 1209-1220.

Mott, K.A. and Woodrow, I.E. (2000) Modelling the role of Rubisco activase in limiting non - steady - state photosynthesis. *J Exp Bot*, **51**, 399-406.

Nixon, P.J., Michoux, F., Yu, J.F., Boehm, M. and Komenda, J. (2010) Recent advances in understanding the assembly and repair of photosystem II. *Annals of Botany*, **106**, 1-16.

Perdomo, J.A., Degen, G.E., Worrall, D. and Carmo-Silva, E. (2019) Rubisco activation by wheat Rubisco activase isoform 2β is insensitive to inhibition by ADP. *Biochemical Journal*, BCJ20190110.

Pignon, C.P., Jaiswal, D., McGrath, J.M. and Long, S.P. (2017) Loss of photosynthetic efficiency in the shade. An Achilles heel for the dense modern stands of our most productive C-4 crops? *Journal of Experimental Botany*, **68**, 335-345.

Rawson, H.M., Hindmarsh, J.H., Fischer, R.A. and Stockman, Y.M. (1983) CHANGES IN LEAF PHOTOSYNTHESIS WITH PLANT ONTOGENY AND RELATIONSHIPS WITH YIELD PER EAR IN WHEAT CULTIVARS AND 120-PROGENY. *Australian Journal of Plant Physiology*, **10**, 503-514.

Rosenthal, D.M., Slattery, R.A., Miller, R.E., Grennan, A.K., Cavagnaro, T.R., Fauquet, C.M., Gleadow, R.M. and Ort, D.R. (2012) Cassava about-FACE: Greater than expected yield stimulation of cassava (Manihot esculenta) by future CO2 levels. *Global Change Biology*, **18**, 2661-2675.

Sage, R.F. and Seemann, J.R. (1993) Regulation of ribulose-1, 5-bisphosphate carboxylase/oxygenase activity in response to reduced light intensity in C4 plants. *Plant Physiology*, **102**, 21-28.

Salter, W.T., Merchant, A.M., Richards, R.A., Trethowan, R. and Buckley, T.N. (2019) Rate of photosynthetic induction in fluctuating light varies widely among genotypes of wheat. *Journal of Experimental Botany*, **70**, 2787-2796.

Sinclair, T.R., Rufty, T.W. and Lewis, R.S. (2019) Increasing Photosynthesis: Unlikely Solution For World Food Problem. *Trends Plant Sci*.

Soleh, M.A., Tanaka, Y., Kim, S.Y., Huber, S.C., Sakoda, K. and Shiraiwa, T. (2017) Identification of large variation in the photosynthetic induction response among 37 soybean Glycine max (L.) Merr. genotypes that is not correlated with steady-state photosynthetic capacity. *Photosynthesis Research*, **131**, 305-315.

Soleh, M.A., Tanaka, Y., Nomoto, Y., Iwahashi, Y., Nakashima, K., Fukuda, Y., Long, S.P. and Shiraiwa, T. (2016) Factors underlying genotypic differences in the induction of photosynthesis in soybean [Glycine max (L.) Merr.]. *Plant, Cell & Environment*, **39**, 685-693.

Song, Q., Srinivasan, V., Long, S.P. and Zhu, X.-G. (2019) Decomposition analysis on soybean productivity increase under elevated CO2 using 3D canopy model reveals synergestic effects of CO2 and light in photosynthesis. *Annals of botany*.

Song, Q., Yan, L., Quigley, C., Jordan, B.D., Fickus, E., Schroeder, S., Song, B.-H., Charles An, Y.-Q., Hyten, D. and Nelson, R. (2017) Genetic characterization of the soybean nested association mapping population. *The plant genome*, **10**.

Song, Q.F., Zhang, G.L. and Zhu, X.G. (2013) Optimal crop canopy architecture to maximise canopy photosynthetic CO2 uptake under elevated CO2 - a theoretical study using a mechanistic model of canopy photosynthesis. *Funct Plant Biol*, **40**, 109-124.

South, P.F., Cavanagh, A.P., Liu, H.W. and Ort, D.R. (2019) Synthetic glycolate metabolism pathways stimulate crop growth and productivity in the field. *Science*, **363**, 45-+.

SURFRAD (2019) Radiation Data Plots: Earth System Research Laboratory, Global Monitoring Division, National Oceanic & Atmospheric Administration, Department of Commerce, USA.

Tanaka, Y., Adachi, S. and Yamori, W. (2019) Natural genetic variation of the photosynthetic induction response to fluctuating light environment. *Current Opinion in Plant Biology*, **49**, 52-59.

Taylor, S.H. and Long, S.P. (2017) Slow induction of photosynthesis on shade to sun transitions in wheat may cost at least 21% of productivity. *Philosophical Transactions of the Royal Society B-Biological Sciences*, **372**.

Townsend, A.J., Retkute, R., Chinnathambi, K., Randall, J.W., Foulkes, J., Carmo-Silva, E. and Murchie, E.H. (2018) Suboptimal acclimation of photosynthesis to light in wheat canopies. *Plant Physiology*, **176**, 1233-1246.

Von Caemmerer, S. (2000) *Biochemical models of leaf photosynthesis*: Csiro publishing.

Wang, Q.X., Zhao, H., Jiang, J.P., Xu, J.Y., Xie, W.B., Fu, X.K., Liu, C., He, Y.Q. and Wang, G.W. (2017a) Genetic Architecture of Natural Variation in Rice Nonphotochemical Quenching Capacity Revealed by Genome-Wide Association Study. *Frontiers in Plant Science*, **8**.

Wang, Y., Song, Q.F., Jaiswal, D., de Souza, A.P., Long, S.P. and Zhu, X.G. (2017b) Development of a Three-Dimensional Ray-Tracing Model of Sugarcane Canopy Photosynthesis and Its Application in Assessing Impacts of Varied Row Spacing. *Bioenergy Research*, **10**, 626-634.

Winer, J. (2019) Looking in the Wrong Direction for Higher-Yielding Crop Genotypes. *Trends Plant Sci*, **24**, 927-933.

Yamori, W., Masumoto, C., Fukayama, H. and Makino, A. (2012) Rubisco activase is a key regulator of non-steady-state photosynthesis at any leaf temperature and, to a lesser extent, of steady-state photosynthesis at high temperature. *Plant Journal*, **71**, 871-880.

Zhu, X.G., Ort, D.R., Whitmarsh, J. and Long, S.P. (2004) The slow reversibility of photosystem II thermal energy dissipation on transfer from high to low light may cause large losses in carbon gain by crop canopies: a theoretical analysis. *Journal of Experimental Botany*, **55**, 1167-1175.

Figure legends

Fig. 1. Modelled soybean canopy structure and its lighting predicted from ray tracing for a clear sky on Aug 20th 2019, at Champaign, Illinois, USA (40.11 °N). Colors indicate the spatial heterogeneity of the intensity of absorbed light at noon.

Fig. 2. Panel b shows the recorded incident light intensity on Aug. 20th, above the soybean canopy of Fig. 1, which was an intermittently cloudy day. Panel a shows the predicted light intensity for the same day based on sun-earth geometry and an atmospheric transimittance of 0.85, assuming a cloud-free clear sky day. The diurnal light absorption simulated for single pixels on the leaves in the top, middle and bottom of the soybean canopy on the sunny day are shown in panels c, e and g, respectively, and for the cloudy day in panels d,f and h, respectively. .

Fig. 3. The cumulative net CO_2 assimilation of the soybean canopy of Fig. 1 (A_c) on the simulated sunny day (Fig. 2a) and cloudy day (Fig. 2b). The black line the predicted assimilation of CO2 that would occur if photosynthesis responded instantaneously to changes in light with no lags in efficiency. Rca accounts for the losses that result from the lags in activation of Rubisco on shade to sun transitions. STNPQ accounts for the losses that result from lags in relaxation of short-term relaxation of NPQ, and STNPQ+LTNPQ accounts for relaxation of all NPQ. Rca+STNPQ+LTNPQ accounts for lags in both induction and relaxation of NPQ. The simulation starts at dawn (5:30 a.m.), with $A_c = 0$.

Fig. 4. The percentage loss in potential daily canopy photosynthetic net carbon assimilation (A_c) due to losses of efficiency through lags in NPQ relaxation and Rubisco activation, from the simulation of Fig. 3. Blue bars (STNPQ) are the decreases in A_c caused by the short-term NPQ relaxation; Yellow bars (LTNPQ) are the decreases of A_c caused by long-term NPQ (Zhu et al., 2004); Green bars (Rca) are the predicted decreases of A_c due to lags in Rubisco activation. The simulated sunny clear sky day on the left and intermittently cloudy day on the right.

Fig. 5. The effect of genetic variation in the speeds of relaxation short-term NPQ on losses of potential daily net CO_2 assimilation (A_c) in the canopy of Fig. 1. Illustrated are losses in A_c resulting from the average of the measured rates of relaxation of STNPQ for the NAM soybean parent population and for the NAM lines showing the fastest (NAM27) and slowest (NAM23) rate of STNPQ relaxation Dark gray bars are losses predicted for the sunny day (Fig.2a) and light gray for the intermittantly cloudy day (Fig. 2b).

Fig. 6. The effect of genetic variation in the speeds of Rubisco activation on losses of potential daily net CO_2 assimilation (A_c) in the canopy of Fig. 1 using the daily sunlight profiles of Figs. 2a&b. . Measured of three soybean genotype were used (Soleh et al., 2017). Illustrated are NAM23, which showed the fastest activation of Rubisco ($\tau_{Rubisco}$), RC which was average for the population and NAM8 which showed the slowest activation. Dark gray bars are losses predicted for the sunny day (Fig.2a) and light gray for the intermittantly cloudy day (Fig. 2b).

Table Legends

Table 1. Input parameters of the soybean canopy model.

Table 2. Measured NPQ relaxation parameters of soybean (cv. LD11-2170).

Table 3. Rubisco activation parameters estimated by using time course of maximum carboxylation capacity of three selected parents of the soybean NAM population during the induction response (Soleh et al., 2017)

Table 1. Input parameters of the soybean canopy model.

Parameter	Full name	Value	Reference
C_i	Intercellular CO_2 concentration	280 µbar	Environmental input
f_h	Empirical constant in determining the decrease of Fv/Fm for a given I_{int}.	5.1e+5	(Zhu, et al. 2004)
Fv/Fm	Maximum quantum yield of PSII	0.801	Measured
Γ^*	The CO_2 compensation point in the absence of dark respiration	38.6 µbar	(Von Caemmerer 2000)
J_{max}	Maximum electron transport capacity	200 µmol m^{-2} s^{-1}	(Bernacchi et al., 2005)
K_o	Michaelis-Menten constant of Rubisco for O_2	404 mbar	(Von Caemmerer 2000)
K_c	Michaelis-Menten constant of Rubisco for CO_2	248 µbar	(Von Caemmerer 2000)
k_{aRac}	A constant for the calculation of maximum steady-state Rubisco activity (eqn.2)	12.4 mg m^{-2}	(Mott and Woodrow 2000)
k_{light}	A constant for the calculation of steady-state Rubisco activity (eqn.3)	120 µmol m^{-2} s^{-1}	(Sage and Seemann 1993)
K_{TaoRac}	A constant for the calculation of the time constant of Rubisco activation	214 min mg m^{-2}	(Mott and Woodrow 2000, Soleh, et al. 2016)
O_2	Intercellular O_2 concentration	210 mbar	Environmental input
PqE	Proportion of the contribution	0.7	Measured

	of *qE* in steady state ΦNPQ		
PqM	Proportion of the contribution of *qM* in steady state ΦNPQ	0.3	Measured
[Rac]	Amount of Rubisco activase	70 mg m^{-2}	(Mott and Woodrow 2000)
R_d	Mitochondria respiration	1.2 µmol m^{-2} s^{-1}	Measured
Temp	Leaf temperature	25 °C	Environmental input
τ_{qE}	Time constant of *qE* relaxation	0.56 min	Measured
τ_{qM}	Time constant of *qM* relaxation	16.8 min	Measured
V_{max0}	Maximum Rubisco activity	120 µmol m^{-2} s^{-1}	(Bernacchi *et al.* 2005)

Table 2. Measured NPQ relaxation parameters of soybean (cv. LD11-2170).

Parameters	**Soybean**
Fv/Fm	0.801 ± 0.032
Φ_{qE}	0.318 ± 0.016
Φ_{qI}	0.097 ± 0.015
Φ_{qM}	0.066 ± 0.008
τ_{qE}*(min)*	0.558 ± 0.051
τ_{qM}*(min)*	16.826 ± 9.134

Table 3. Rubisco activation parameters estimated by using time course of maximum carboxylation capacity of three selected parents of the soybean NAM population during the induction response (Soleh et al., 2017)

Parameters	**NAM23**	**RC**	**NAM8**
a (µmol m^{-2} s^{-1})	72.2	80.0	85.0
c (µmol m^{-2} s^{-1})	21.6	17.3	7.6
$\tau_{Rubisco}$ (s)	129.7	471.7	1850.0
R^2	0.982	0.977	0.976

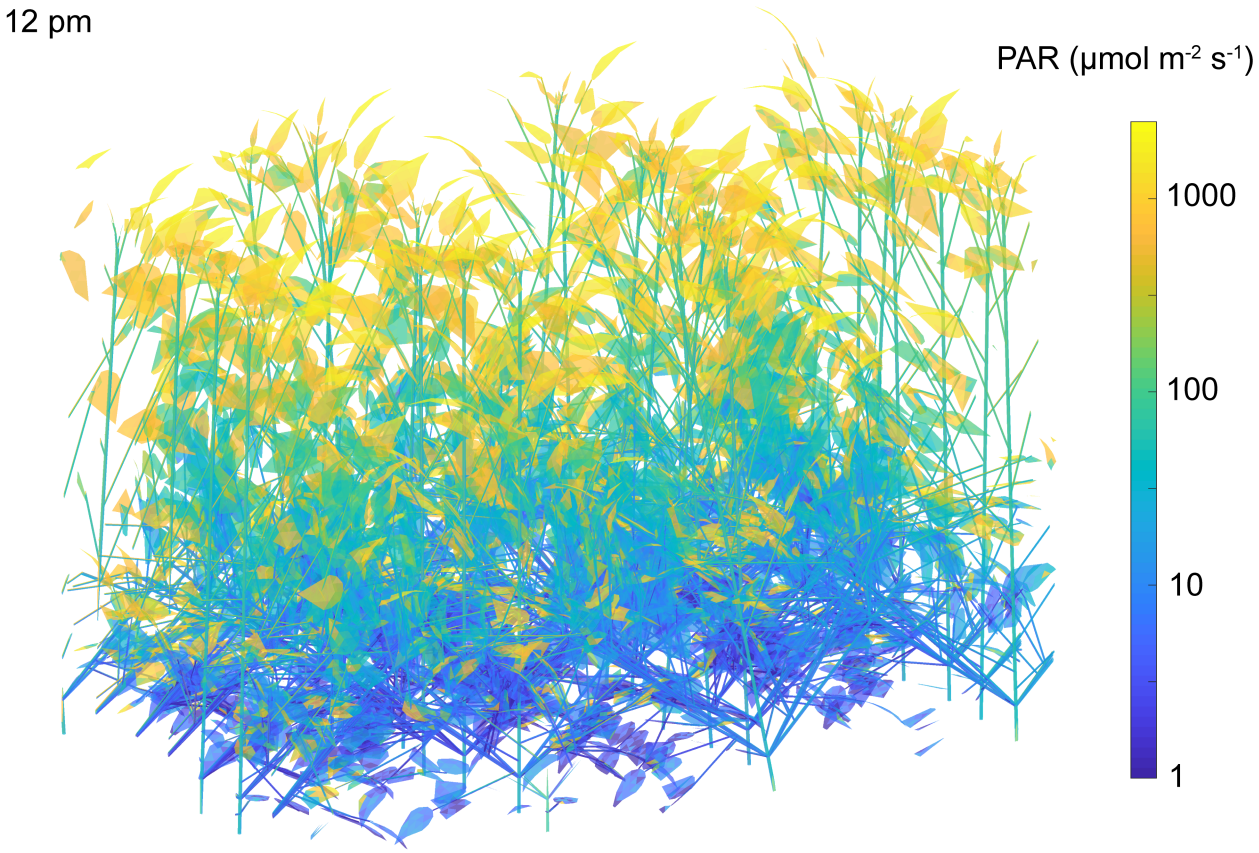

tpj_14663_f1.tif

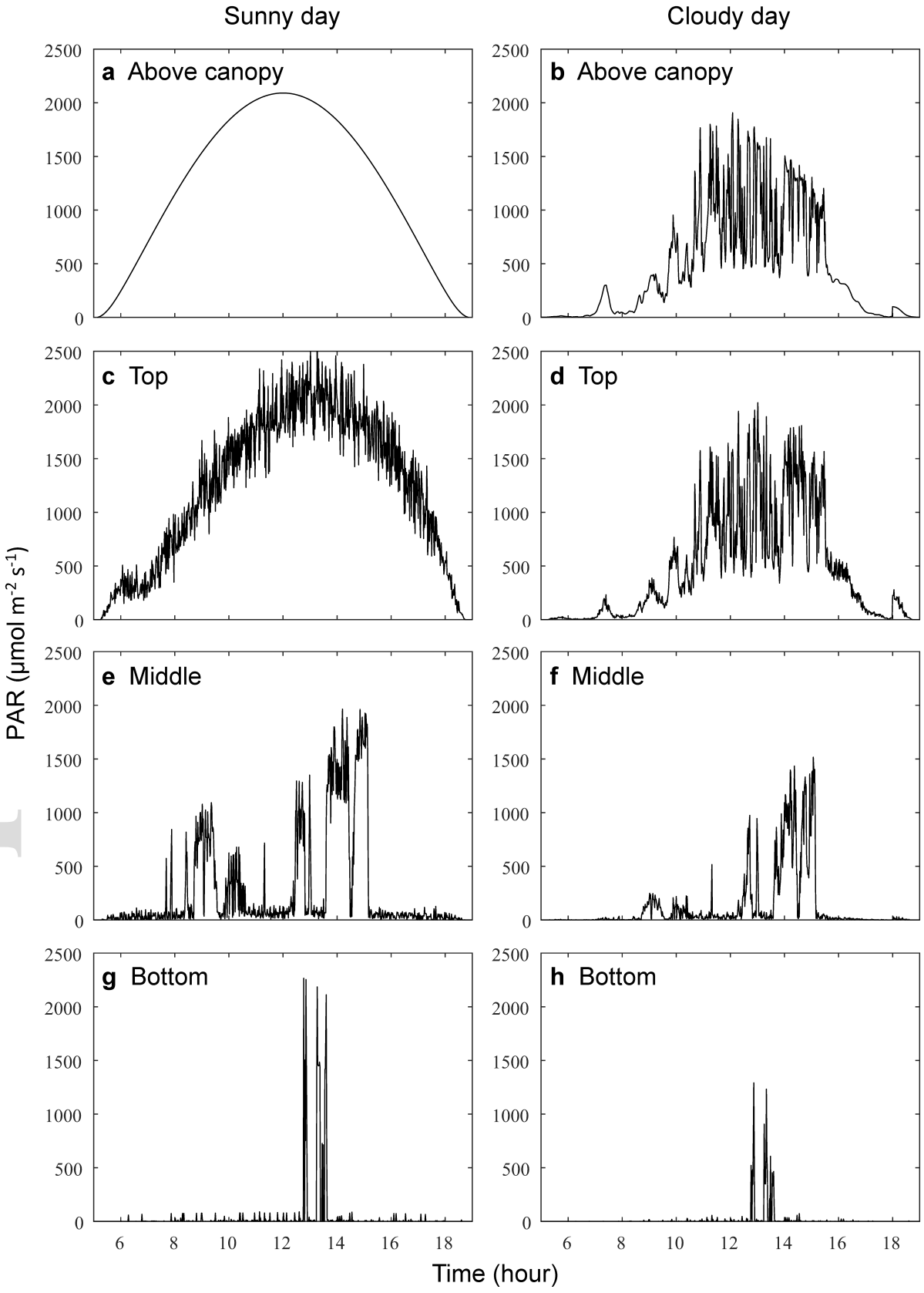

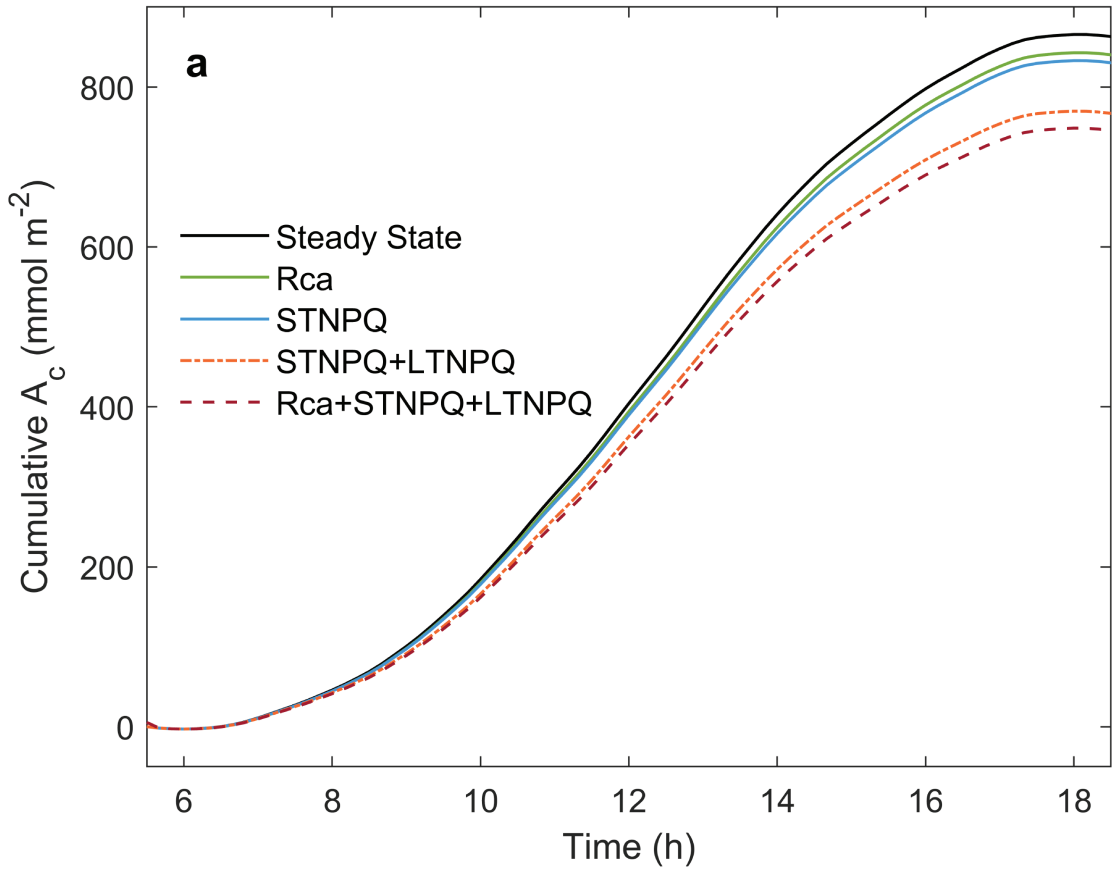

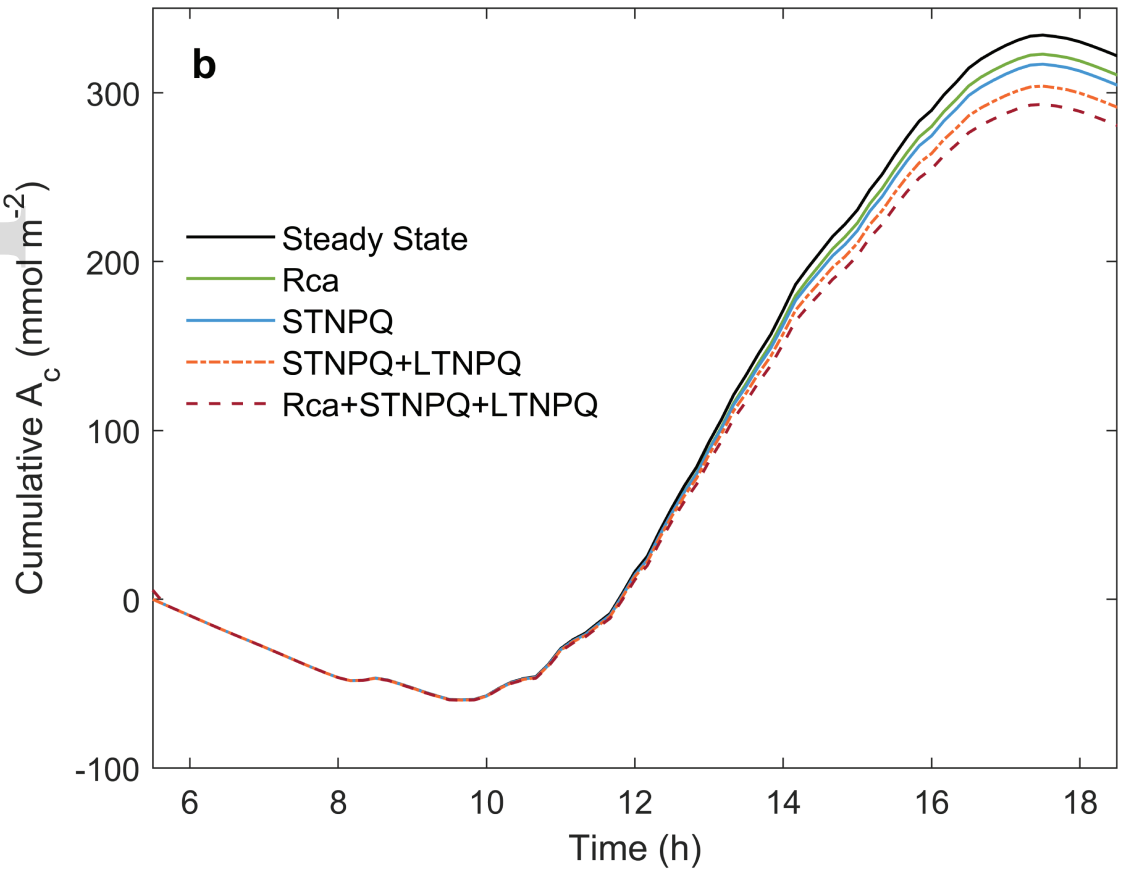

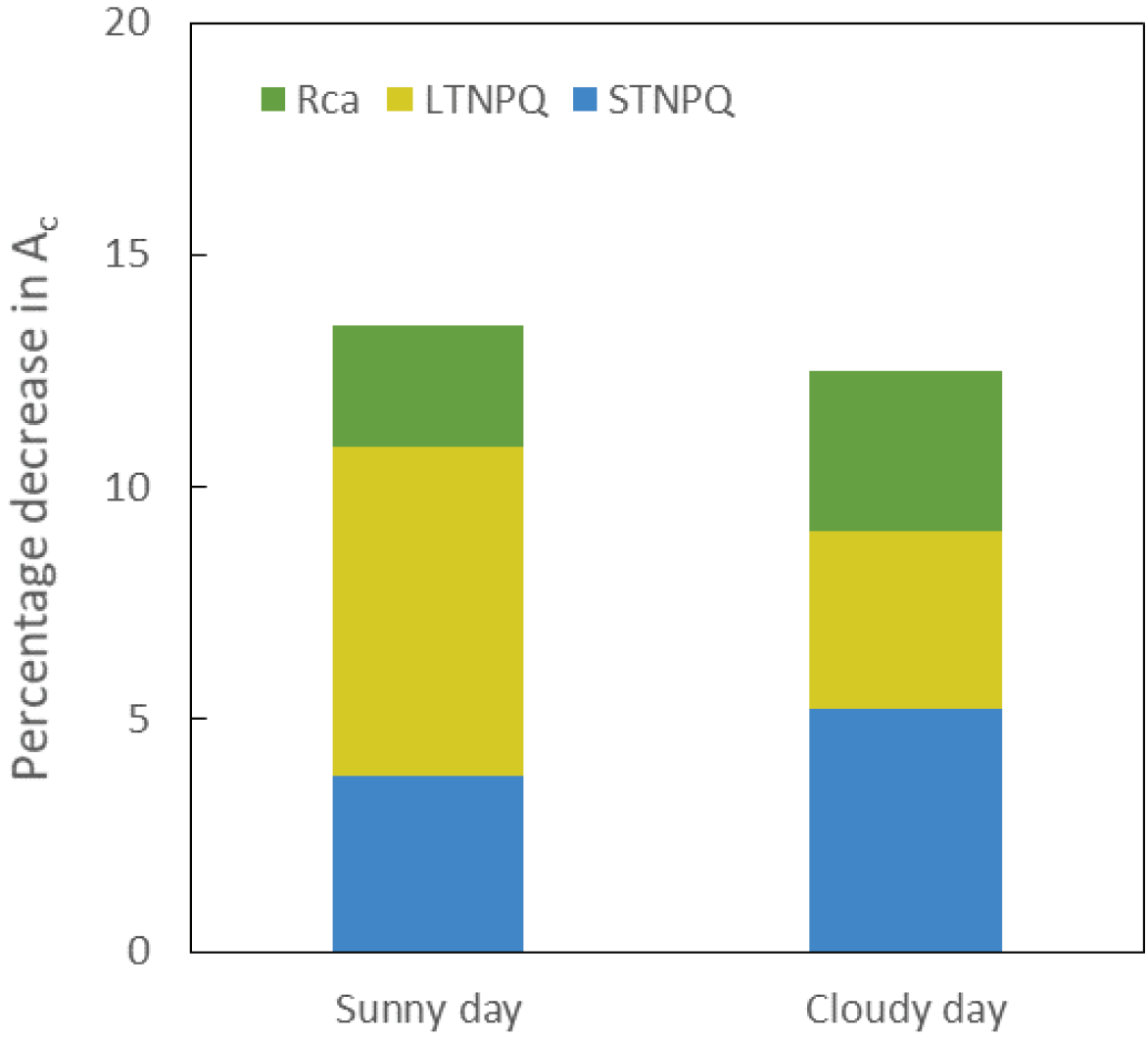

tpj_14663_f4.tif

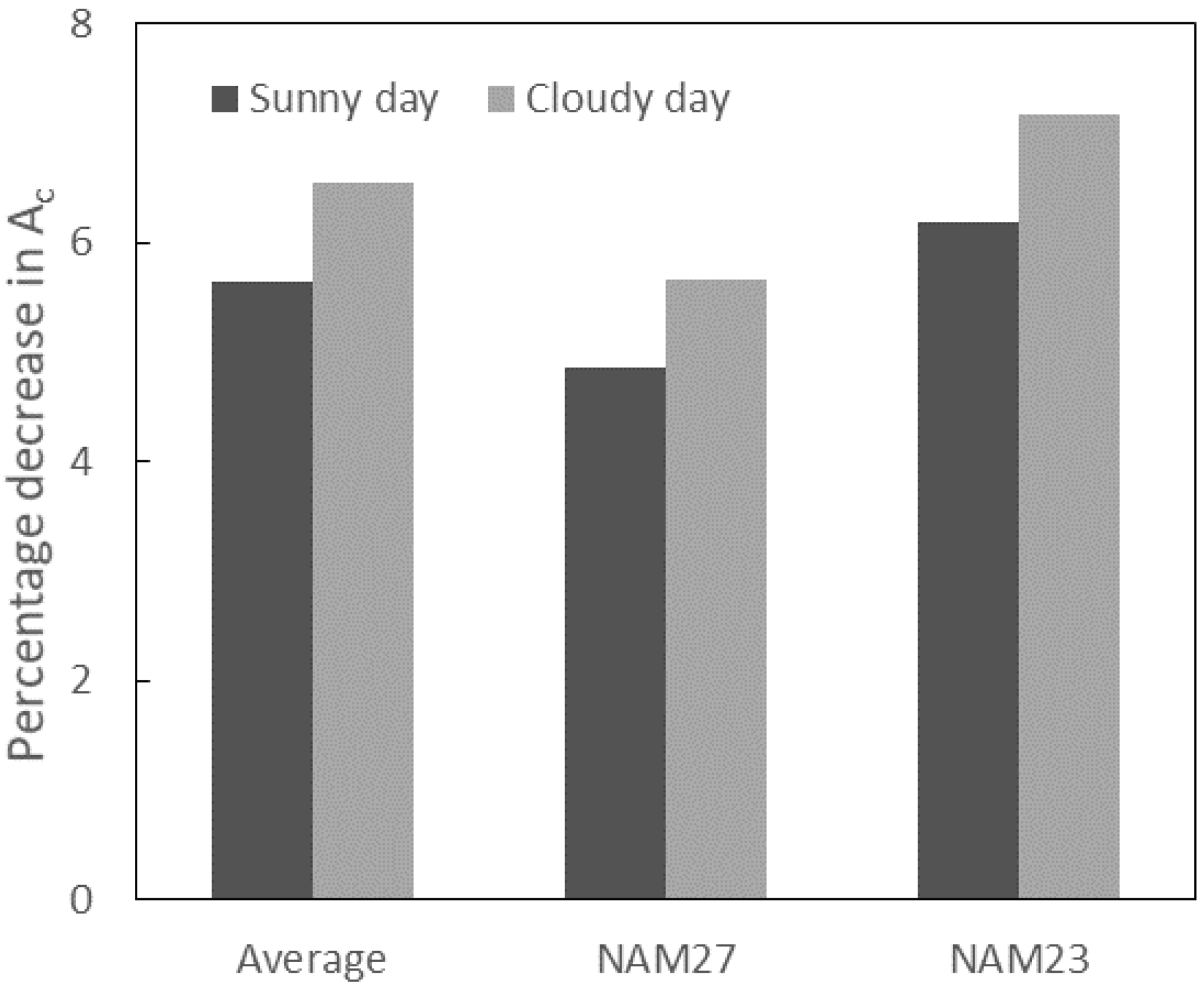

tpj_14663_f5.tif

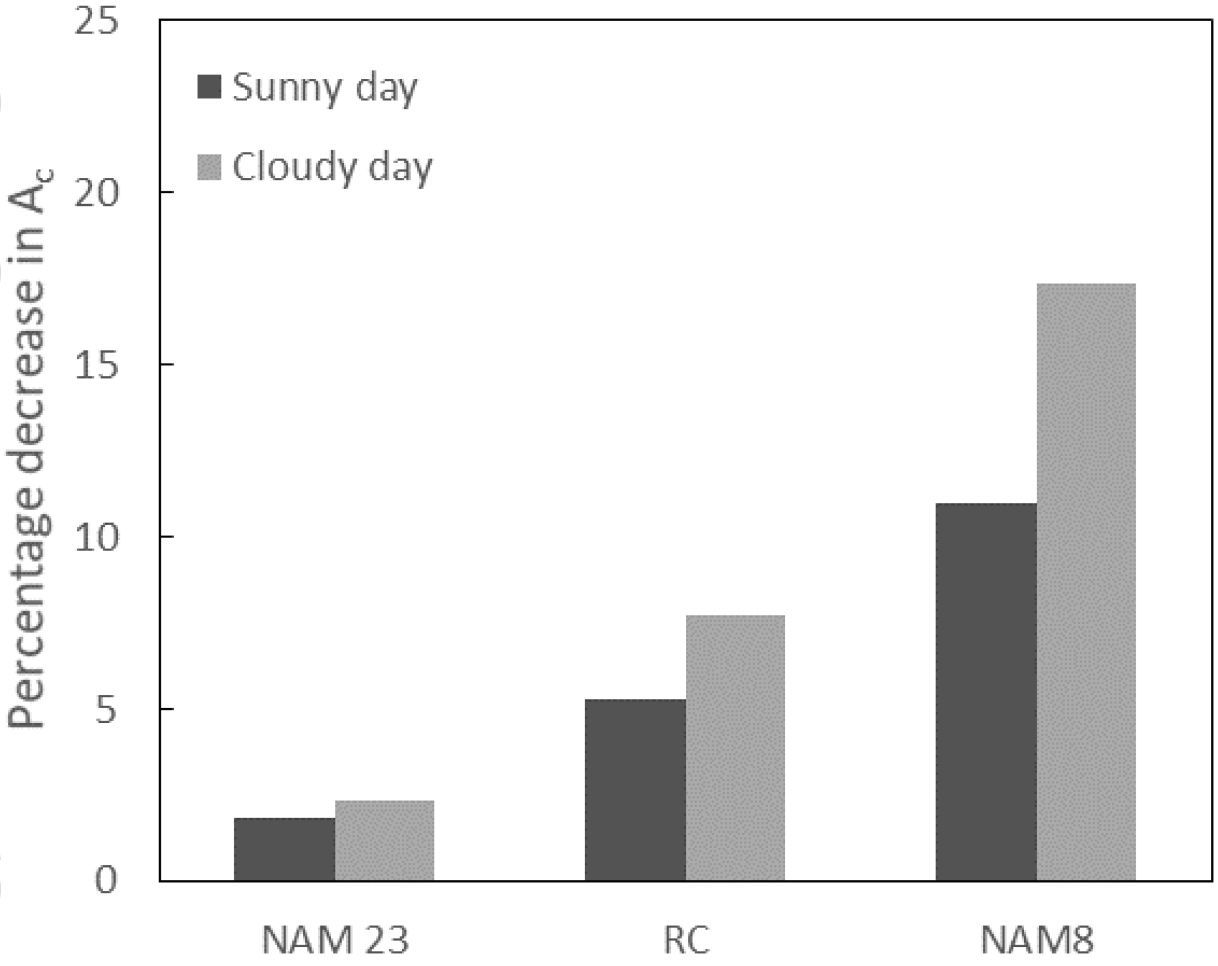

tpj_14663_f6.tif